Chapter II

Synthetic Approaches to Homo- and Multi-Material Nanocrystals

2.1 Introduction

In the previous chapter the size and shape dependence of the chemical and physical properties of colloidal nanocrystals (NCs) has been presented. It appears clear that precise control of compositional and geometric features allows not only observation of the unique properties of NCs, but also their tuning, as desired.

As of today, many methods are available to fabricate NCs, including, on one side, physical approaches, such as those involving epitaxial growth of "islands" on substrates through a molecular beam (Molecular Beam Epitaxy) or extrusion of nanostructures from bulk targets (Laser Ablation) and, on the other side, chemical routes, such as those achieving nanomaterial deposition from reaction of metal-organic species in the gas phase (Chemical Vapor Deposition) or formation of free-standing nanoparticles in liquid media in the presence of organic stabilizers (wet-chemical synthesis). Among wet-chemical methods, the colloidal approach has been proven to be a particularly successful means of achieving easily processable NCs with tailored crystalline structure and narrow distribution of sizes and shapes. As these routes will be the main subject of this thesis, the basic principles underlying their operation will be highlighted in this chapter.

In the colloidal synthesis, the growth medium is a liquid mixture of ligands or surfactants and the whole synthesis process is usually carried out under inert atmosphere (**Fig. 2.1a**). The surfactants commonly used in colloidal syntheses include alkyl thiols, amines, carboxylic and phosphonic acids, phosphines, phospine oxides, phosphonates, phosphates and various coordinating solvents, such as ethers or alkenes. ¹⁻⁵ In general, the molecular precursor species are introduced into the reactor via a fast injection into the pre-heated mixture of surfactants or are mixed with the other reagents and heated up to a target temperature, depending on the growth mechanism of the specific NC system. ⁶⁻⁸ The decomposition of precursor species generates reactive species, henceforth broadly referred to as the "monomers", which often form complexes with the surfactants or ligands. ⁶⁻¹⁰ The steep rise in monomer concentration that follows precursor decomposition induces a burst of nucleation, which is then followed by the growth of the initially formed nuclei (**Fig. 2.1b**). ¹⁻⁵ During the synthesis, surfactants and ligands play a key role in tuning the reactivity of the monomers, and in regulating the evolution of the NC size over time in a controlled way, as they are continuously absorbing and

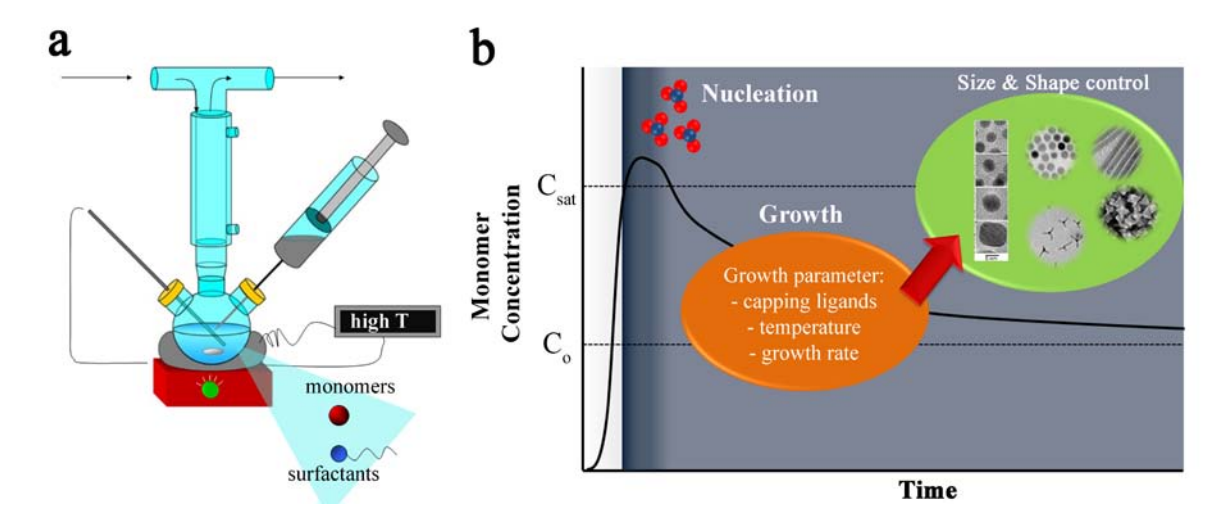


Figure 2.1 (a) Sketch of a typical reactor used for wet-chemical colloidal synthesis. (b) La Mer diagram of crystal nucleation and growth. When the monomer concentration reaches the supersaturation threshold (C_{sat}), nucleation occurs, after which monomers continue to add to the as-formed nuclei seeds during the growth stage, resulting in a gradual decrease of monomer concentration down to the solid/solution equilibrium value (C_{o}). (adapted from ref. 1)

desorbing from the surface of the NCs through their polar head groups, allowing the addition/removal of chemical species. When the synthesis is stopped by lowering the reaction temperature, a surfactant coating remains tightly bound to the surface of the NCs and guarantees their solubility in a variety of solvents. In addition, as already mentioned in the first chapter, not only size and shape, but also surface passivation by surfactants may influence the properties of colloidal NCs. ¹¹⁻¹⁴

Details on the nucleation and growth processes underlying the formation of NCs will be given in the next sections of this chapter.

2.2 Homogeneous nucleation of nanocrystals

Homogeneous nucleation takes place in the absence of any pre-existing condensed phase. In order to form the nuclei, the system will need to overcome an energy barrier. The latter is related to the fact that a new interface needs to be formed between the solution and the new phase. From a thermodynamic point of view, the nucleation event can burst when the chemical potential of the species in the solution, μ_{sol} , equals the chemical potential of the same species in the crystal, μ_{cryst} . Figure 2.2 reports the different dependence of the two potentials on the concentration of monomer species. When the concentration of monomers in solution overcomes the equilibrium value, C_0 , the system will be in a metastable state, where the chemical species are not stable any more in the liquid phase and would tend to form a new condensed phase. The system persists in this state with actually no nucleation taking place yet, until a critical value of supersaturation, C_{sat} , is crossed (Fig. 2.1b). Once passed this, nucleation proceeds at a considerable rate. The critical supersaturation value depends on many parameters, such as for instance, the temperature and the interfacial energy between the solid and the solution phase. The interfacial energy can be modified considerably by the presence of surface-adhering ligands, which can in turn affect significantly the reactivity of the NCs toward the monomer species approaching the crystal from the solution.

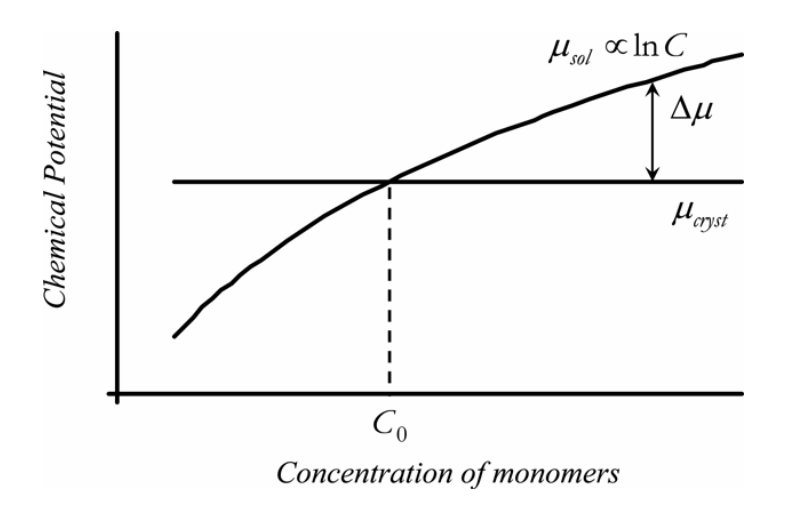


Figure 2.2 Simplified diagram showing the trend of the chemical potential of the monomers: μ_{sol} is the chemical potential of monomers in solution; μ_{cryst} is the chemical of the same species in the crystal phase; C_0 is the monomer concentration in the correspondence of which $\Delta \mu = \mu_{sol} - \mu_{cryst} = 0$.

More in detail, according to the Classical Nucleation Theory (CNT) ¹⁵, the free energy required for nuclei formation, ΔG_{hom} , is described by the following equation:

$$\Delta G_{\text{hom}} = \Delta G_V + \Delta G_S \tag{2.1}$$

where:
$$\Delta G_V = -n \times \Delta \mu = -\frac{V}{v} \Delta \mu = -\frac{4\pi r^2}{3v} \Delta \mu \qquad (2.2)$$

and
$$\Delta G_S = 4\pi r^2 \gamma_{Nl} \tag{2.3}$$

 ΔG_V is referred to as the "volume term", since it scales with the size of the nuclei (Eq. 2.2). It is the chemical potential gained by the formation of a new spherical nucleus of radius r and volume $V=4/3 \, m^3$, which contains n moles of the monomers and is characterized by a molar volume, v.

 ΔG_s is a "surface energy term", which represents the free energy that must be spent in order to establish the new interface between the new solid phase and the pre-existing solution phase. This term scales with the interfacial area, which is $4\pi r^2$ in the case of a spherical nucleus of radius r, and with the interfacial energy per unit surface area (i.e. surface tension), γ_{Nl} .

By combining the two expressions above for ΔG_V (Eq. 2.2) and ΔG_S (Eq. 2.3), the total free energy for the homogeneous nucleation in the hypothesis of spherical nuclei can be written as:

$$\Delta G_{\text{hom}} = \frac{4\pi r^2}{3\nu} \Delta \mu + 4\pi r^2 \gamma_{Nl}$$
 (2.4)

The general trend of the free energy versus the radius of the forming nuclei is reported in **Fig. 2.3.** The point of maximum in the ΔG_{hom} curve is the activation barrier, ΔG_{hom}^* , that the system must overcome in order for nucleation to be triggered. The r value in the correspondence of the activation barrier, r^* , is called the "critical radius". If a nucleus is just slightly larger than r^* , it will "roll" toward a lower value of ΔG_{hom} , where its stability will be higher, and it will continue to grow (**Fig. 2.3a**). On

the contrary, a nucleus that has not been able to reach r^* will shrink and disappear, since it will reduce its overall free energy of formation by reducing the size (**Fig. 2.3a**).

In addition, depending on the monomer concentration and consequently on the supersaturation level (**Fig. 2.2**) realized in the reactor, the critical size will change (**Fig. 2.3b**). For higher supersaturation values, the critical radius is smaller and the energetic barrier for nucleation is also low. This means that proportionally small crystals will be stable in solution and a large percentage of them will have the chance to grow further after the nucleation stage (**Fig. 2.3b**).

Besides by the monomer concentration, the supersaturation is influenced by the temperature. Indeed, as temperature increases, the molecular volume v increases, while the surface tension generally decreases. The temperature dependence of these two parameters, both of which are involved in Eq. 2.4, implies that higher reaction temperatures decrease the energetic barrier for nucleation, thereby favoring the formation of smaller nuclei.

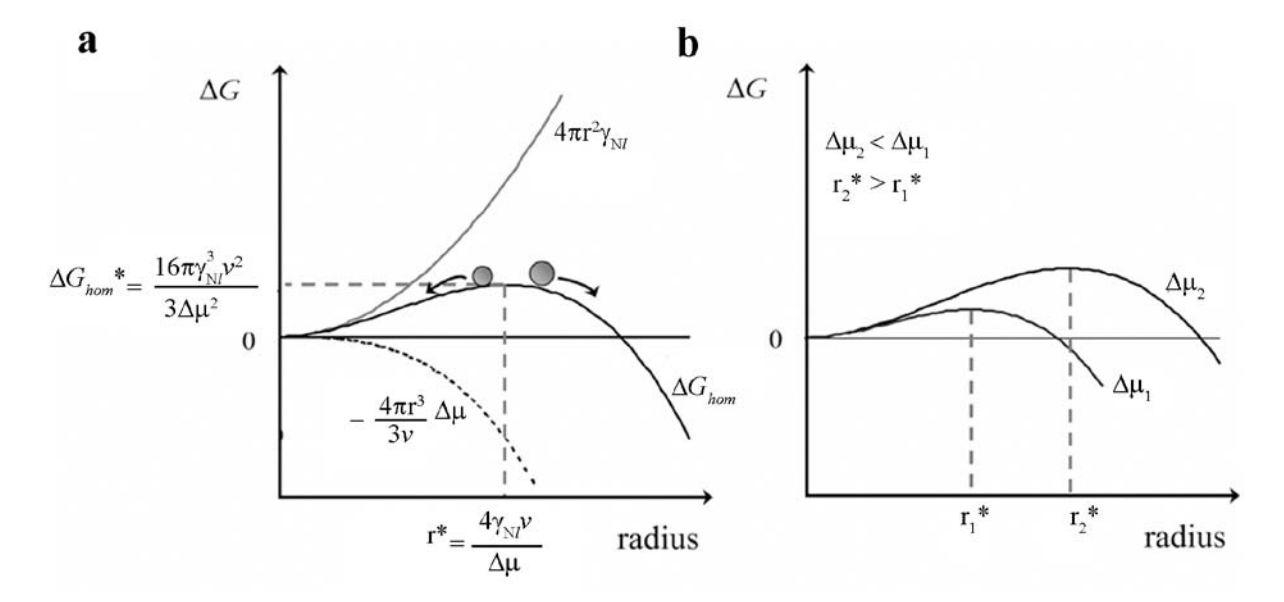


Figure 2.3 (a) Plots of the different contributions to the overall free energy ΔG . (b) Dependence of the critical size and of the energetic barrier for nucleation on supersaturation.

2.3 Heterogeneous nucleation of nanocrystals

Heterogeneous nucleation occurs when NCs nucleate on pre-existing crystals, named *nucleation seeds*. The two crystals, the one to be grown and the pre-existing one, can be of the same chemical nature or be different from each other. As sketched in **Figure 2.4a** three types of interfacial energies have to be considered: i) the tension at the nucleus-liquid solution interface, γ_{Ni} ; ii) the tension at the nucleus-substrate interface, γ_{NS} ; iii) the tension at substrate-solution interface, γ_{SI} . The angle θ at the three-boundary region is an important parameter defining the wettability of the substrate seed by the "heterogeneous nucleus". Depending on the wettability, θ can vary from 0 (complete wettability), meaning that the substrate and the nucleus are made of the same material, and π (complete lack of

wettability), implying that heterogeneous nucleation does not occur. According to the CNT, the overall free energy of heterogeneous nucleation can be written as:

$$\Delta G_{het} = -\frac{V_{het}}{v} \Delta \mu + \gamma_{Nl} A_{Nl} + \gamma_{NS} A_{NS} - \gamma_{Sl} A_{Sl}$$
 (2.5)

In **Figure 2.4b** the dependence of the total free energy of heterogeneous nucleation on the radius is shown.

Interestingly, the relationship that can be extracted between the activation energies for homogeneous and heterogeneous nucleation, ΔG_{hom}^* , and ΔG_{het}^* , is the following:

$$\Delta G_{\text{hef}}^* = f(\theta) \Delta G_{\text{hom}}^*$$
 where $0 < f(\theta) < 1$ (2.6)

 $f(\theta)$ is the contact parameter that is zero in the case of complete wettability and equal to 1 in the case of non-wettability.

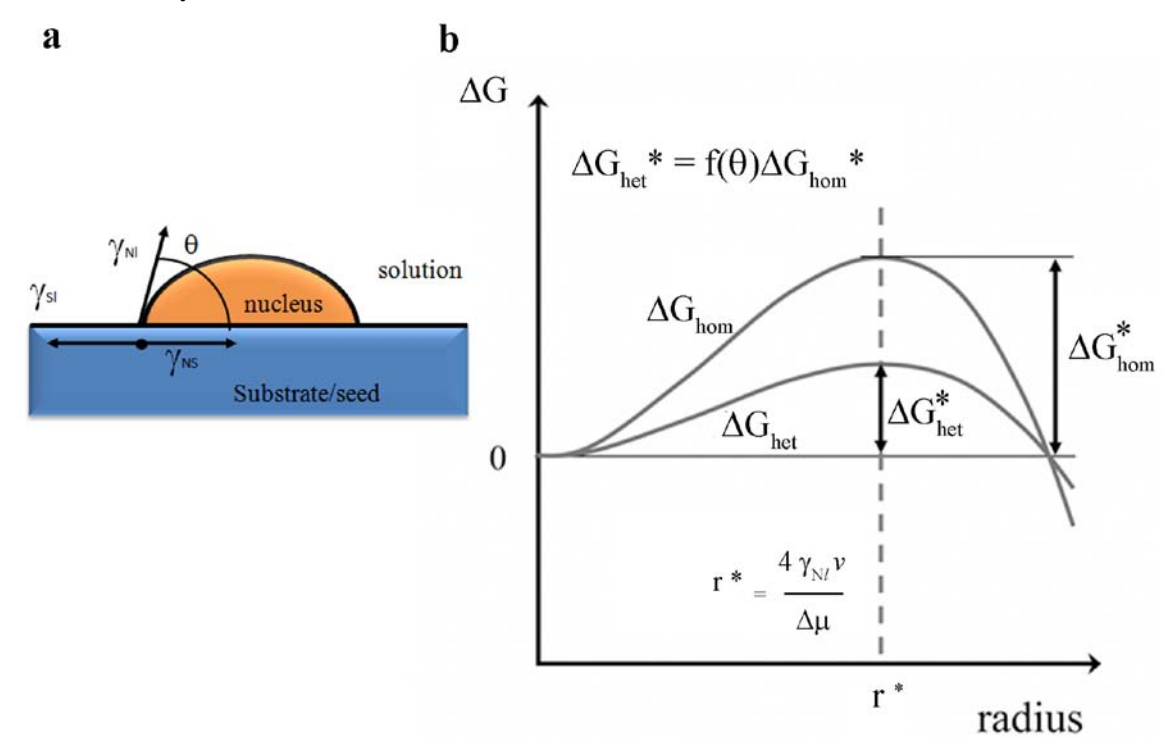


Figure 2.4 (a) Sketch of a heterogeneous nucleus deposited on a flat substrate/seed. The relevant parameters involved in the classical nucleation theory of heterogeneous nucleation have been reported. (b) Comparison between homogeneous nucleation and heterogeneous nucleation

The main conclusion that can be drawn is that the energetic barrier for heterogeneous nucleation is always lower than that required by homogeneous nucleation, so that in the presence of preformed seeds the secondary material can be expected to prefer nucleating on them rather than separately in the bulk solution.

2.4 Nanocrystal growth

In this section the growth stage of NCs will be discussed. At first it should be considered that not all the monomers in solution are consumed during the nucleation stage. As soon as the nuclei start forming and many of them are able to grow beyond the r^* size threshold, the amount of free unreacted monomers in solution will drop considerably, and this will rapidly raise the barrier for the formation of new stable small nuclei. From this moment on, almost exclusive growth of the nuclei will occur via diffusion of monomers to the proximity of the NCs and subsequent reaction at their surface. The limiting step in NC growth can be either the diffusion of monomers (the so-called diffusion-limited regime) or the reaction rate of monomers at the NC surface (the so-called reaction-limited regime).

Most frequently, soon after the nucleation, the monomer concentration in solution is still high, so that growth will be "reaction-controlled". In this regime the rate-limiting step is the reaction rate of monomers at the surface of the NCs, which proceeds whenever there is a free site for their incorporation into a growing crystal. The growth rate can be expressed as a function of the rate at which n monomers are incorporated in the NC per surface area, dn/dt:

$$\frac{dr}{dt} = \frac{1}{4\pi r^2 d_m} \frac{dn}{dt} \tag{2.7}$$

where d_m denotes the density of monomers in the crystal, thus the inverse of the volume occupied by one monomer.

Over time, monomers are slowly depleted in solution, and the growth rate is dictated by the rate at which monomers reach the surface of the NCs. As the diffusion process becomes unable to replenish the monomers that are rapidly reacting at the NC surface, a linear monomer concentration gradient starts to be built up across the solution layer surrounding the NC surface (the so-called "diffusion layer"). In this situation the growth limiting step is the supply of monomers to the surface of the NCs and the system is said to be "diffusion-controlled". Herein, the expression representing the growth rate of NCs is:

$$\frac{dr}{dt} = \frac{K}{r} \left(\frac{1}{r} - \frac{1}{r} \right) \tag{2.8}$$

where K is a constant that includes various kinetic and thermodynamic terms, among which the diffusion coefficient, and δ is the thickness of the diffusion layer around the particle, r is the NC radius, and r^* is the critical size. From equation (2.8), represented graphically in **Figure 2.5** it can be

deduced that: (i) if
$$r = r^*$$
, $\frac{dr}{dt} = 0$; (ii) if $r < r^*$, $\frac{dr}{dt} < 0$: the NCs will shrink; if $r > r^*$, $\frac{dr}{dt} > 0$: the NCs will grow.

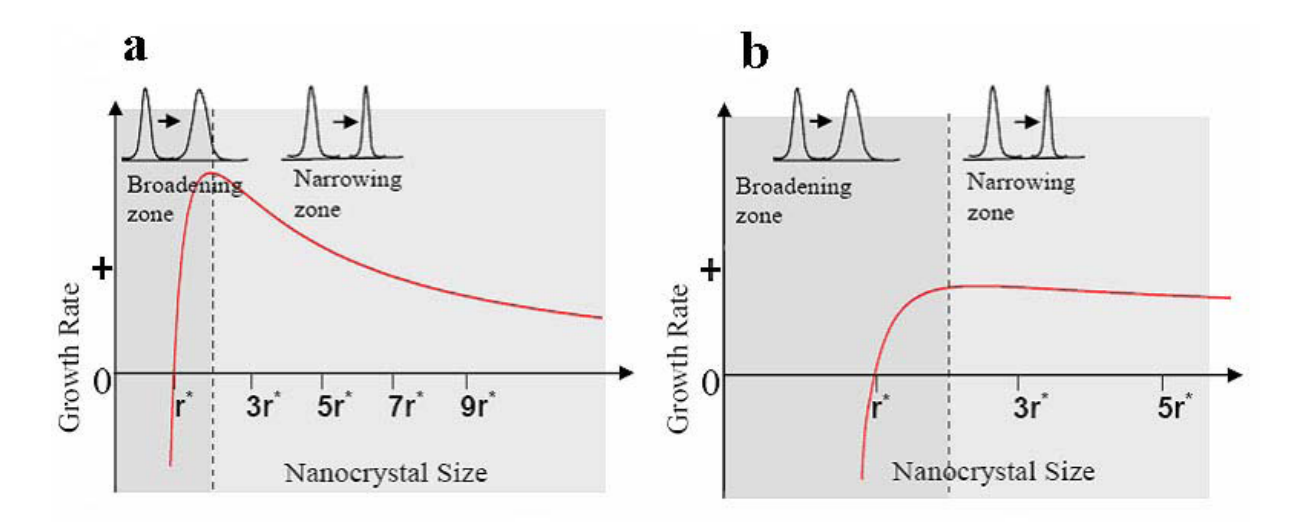


Figure 2.5 Sketch depicting the growth rate of nanocrystals as a function of their size in different stages of the diffusion-limited growth regime. Both curves exhibit a maximum corresponding to the critical radius r^* , which increases with growth proceeding from (a) to (b). During the earlier growth stages (a), most nuclei will exceed r^* and will be in the size-distribution narrowing regime. On the other hand, at longer reaction times (b) the probability of size-distribution broadening is much higher.

Since all NCs follow a similar growth mode, the initial size distribution σ_0 is largely determined by the time over which the nuclei are formed. To study the time dependence of the size distribution, it is useful to derive Eq. 2.8. Then the rate at which Δr (the difference between the smallest and the largest size in the solution) changes with the time is given by the following expression:

$$\frac{d\Delta r}{dt} \approx \frac{k\Delta r}{r_{mean}^2} \left(\frac{2}{r_{mean}^2} - \frac{1}{r} \right) \tag{2.9}$$

where r_{mean} is the geometric mean radius of the NCs.

When the system enters the diffusion-limited regime, r^* is still small, since the concentration of monomers is still quite high, and the growth rate is satisfactory represented by the curve in **Figure 2.5a**. From Eq. 2.9, it can be drawn that for $r_{mean} > 2r^*$ the growth rate decreases with increases in the NC size. This means that small NCs will grow faster then the bigger ones, leading to a *focusing regime*, in which the size distribution tends to narrow. On the contrary, if $r_{mean} < 2r^*$ the system will be in a *de-focusing regime*, since bigger NCs will have a higher growth rate. ¹⁶ Over time the monomer concentration drops and r^* increases (**Fig. 2.5b**). This implies an expansion of the de-focusing window, therefore it is more likely for the size distribution to fall in this zone.

As the reaction goes on, r^* increases further, until eventually the growth rate for the smallest NCs becomes negative (i.e., they start dissolving). In this so-called *Ostwald ripening* regime, the larger NCs are fed with the monomers released to the solution upon dissolution of smaller NCs. From this moment on, the size distribution broadens at a much faster rate than in any of the previous growth stages.

2.5 Size Control

In general, a separation between the nucleation and the growth step is desirable in order to obtain relatively monodisperse samples, meaning that nucleation should occur on a short time scale. ¹⁶ This may be achieved by rapidly injecting suitable precursors into a solvent pre-heated at high temperature to generate a temperature drop in the solution concomitant to the induction of nucleation (the so-called "hot-injection technique"). ^{7, 16, 17} Since the nucleation rate is much more sensitive to changes in temperature compared to the growth rate (see **Eq. 2.10**), the hot-injection allows a temporal separation of nucleation and growth. Indeed, homogeneous nucleation can be completely quenched via a small temperature drop, whereas the growth rate undergoes less drastic changes.

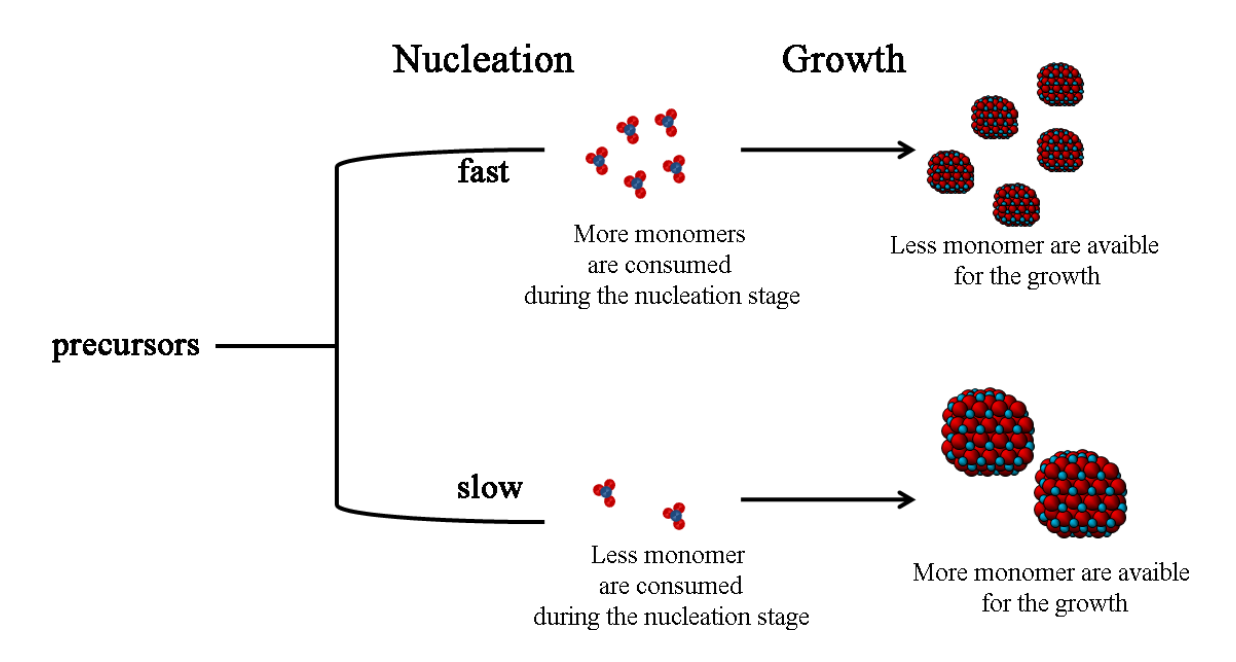
Interestingly, a rapid precursor injection is not the only means of leading to a short nucleation event. For example, in the case of iron oxide grown in hot surfactant mixtures, the injection of the iron pentacarbonyl precursor is followed by a long incubation time before a sudden burst of nucleation takes place.^{8, 18, 19} This "delayed nucleation" is caused by a gradual transformation of iron–surfactant complexes into intermediate species (iron oxo clusters) acting as monomers.¹⁹⁻²² Because the nucleation rate depends exponentially (**Eq. 2.10**) on the monomer concentration, a brief shoot of nucleation occurs when the nucleation threshold is surpassed. The nucleation event depletes the monomer concentration, and subsequent growth occurs with no further nucleation taking place along.

Regarding the control of the NC size, it can be influenced by many synthetic parameters. Herein, the influence of temperature, monomer concentration and surfactant type/concentration will be briefly discussed, although the effects of these parameters are strictly interconnected. According to the CNT the crystal nucleation rate per unit volume, J_N , is:

$$J_N = B_N \exp\left(-\frac{\Delta G_{\text{hom}}^*}{RT}\right) \tag{2.10}$$

where ΔG_{hom}^* is the nucleation activation energy and B_N is a pre-exponential factor depending on many parameters, such as the solvation of species. This equation predicts that at higher temperatures the nucleation is faster, so that more monomers are consumed during the nucleation stage and relatively smaller NCs are ultimately obtained. This is because the nuclei have to compete more for the monomers left in the solution after the nucleation burst (**Scheme 2.1**).^{17, 23} Generally, this holds true for systems in which monomers form instantly upon introduction of precursors into the reaction mixture.

Anyway, a careful control on the reactants in the reaction medium is required, since the generation of an exceedingly high monomer concentration could imply undesired overlapping between the nucleation and the growth stages with a consequent broadening of the size distribution. One possible way to extend NC growth while avoiding this problem is by keeping the concentration of monomers to a constantly low level over the synthesis course. This can be achieved, for example, by performing a slow addition of extra precursors at suitably scheduled time intervals following the initial injection.



Scheme 2.1. Schematic representation of nanocrystal size control depending on the nucleation rate and on the relative fraction of monomers consumed between the nucleation and growth stages (adapted from ref. 17)

Constantly low concentration of monomers favors preferential enlargement of the pre-existing nuclei or seeds over undesired homogeneous nucleation, which remains energetically disfavored instead. ^{21, 24, 25}

In the simplest case in which surfactants act only as dynamic binders (soft templates) on the NC surface, their concentration, their adhesion strength and steric hindrance will play important roles in NC size control. As a consequence of the adsorption/desorption equilibrium of the surfactants on the NCs, regions of their surface are transiently accessible to monomer incorporation. However, ingrowth NCs are, on average, protected by a mono-layer of organic ligands that prevent irreversible interparticle aggregation. It is easy to understand that high surfactant concentration or ligands acting as very strong binders or being characterized by a high steric hindrance will prevent the further addition of monomers for NC growth, leading to relatively smaller nanoparticles in the most systems. ²⁶⁻³⁰

2.6 Shape control

The final geometry of NCs is determined by several mechanisms occurring during the nucleation and growth processes. Initially the crystal phase in which the NC seeds are attained at the nucleation stage is the critical parameter for directing NC shape due to development constraints associated with the symmetry characteristics of the unit cell structure. During growth, several other factors may affect NC shape evolution. Such key factors include the intrinsic surface energy of different crystallographic surfaces, the adhesion of surface-selective capping molecules, and the switching of the NC growth between regimes governed by either thermodynamic factors or kinetic processes. By changing the synthesis parameters, systematic manipulation of these mechanisms is possible, which can ultimately afford various symmetry-controlled NCs.^{1-5, 31, 32}

2.6.1 Control of the growth regime: thermodynamics vs. kinetics

One major issue underlying shape determination is the delicate balance between the kinetic and thermodynamic factors (**Fig 2.6**). Under a thermodynamically controlled growth, which is characterized by a sufficient supply of thermal energy and low fluxes of incoming monomers, NCs with isotropic shapes are generally favored, since these are featured by the lowest surface energy. In contrast, under nonequilibrium growth conditions, anisotropic metastable shapes can be obtained (rods, disks, branched objects) for which lattice development is facilitated along the most kinetically favorable directions with low activation barriers for monomer addition (higher chemical reactivity). The control of the growth regime can be achieved by changing the reaction parameters, such as the monomer concentration and the growth temperature. 1-5, 33-37

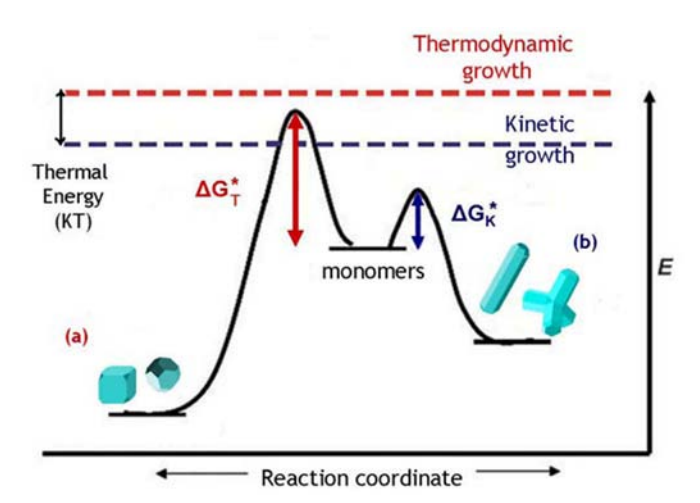


Figure 2.6 Energy diagram comparing nanocrystal growth under thermodynamically and kinetically controlled growth regimes. At high temperatures more symmetric shapes are preferred which are thermodynamically more stable. At lower temperatures and under high reactant fluxes, kinetically overdriven conditions favor more asymmetric shapes, like rods or tetrapods.

2.6.2 Crystal phase effect of nucleating seeds

The seeds nucleated at the early reaction stages can potentially occur in a variety of crystal phases with either highly symmetric (e.g., cubic) or asymmetric structure (e.g., hexagonal, monoclinic). ^{1-5, 31, 32, 36, 38} The most stable phase in which a material nucleates and grows is highly dependent on its environment, such as temperature, capping molecules, chemical potential of monomers in solution. Once the crystal phase is determined at nucleation, the characteristic unit cell structures of the nucleated seeds can strongly affect subsequent NC growth. Usually symmetric crystal structures lead to evolution of isotropic shapes (such as cubes, spheres or polyhedrons), while asymmetric crystal structures can facilitate anisotropic growth along crystallographically nonequivalent lattice directions, resulting in shapes such as disks, ellipsoids, rods and wires. ^{1-5, 31, 32, 36, 38}

An example of how the temperature can affect the seed crystal phase and, consequently, the final NC shape is given by CdS NCs synthesized in alkylamine upon decomposion of a single Cd/S source precursor.^{1, 4, 39} At high temperature (~300°C) CdS seeds form in the hexagonal wurtzite phase and exclusive formation of one-dimensional nanorods is observed. At lower temperatures the symmetric

zinc blend phase is preferred and tetrahedral-shaped seeds enclosed by four equivalent {111} facets form (**Fig. 2.7**). Subsequent growth of wurtzite rods out of the {111} facets leads to the formation of CdS multipods.^{1, 4, 39}

2.6.3 Facet-selective surfactant adhesion mechanism

After the crystal phase of nucleated seeds is determined, one critical parameter governing the final shape is the intrinsic surface energy of the crystallographic facets exposed by the growing seeds. The relation between the respective surface tension and the relative extension of the various crystal facets at the surface of a crystal in thermodynamic equilibrium growth conditions is given by the Wulff construction.^{5, 40} The final crystal shape will be dominated by the facets with lower surface tensions, whereas the higher energy facets will be less extended, or even absent. The relative surface areas associated with the various facets exposed will therefore be such that the total surface energy is minimized. Unfortunately, the Wulff theorem fails to predict the shapes of NCs that are exceedingly small, in which the considerable density of high-energy surface sites, such as corners, edges, and defects, may dramatically affect the overall surface energy balance, unlike in large crystals. Furthermore, it has to be considered that, in most cases, colloidal growth is accomplished under reaction conditions that are quite far from thermodynamic equilibrium. The Wulff theorem, however, has still a strong implication in crystal evolution, if the growth rates of the various facets, rather than their equilibrium surface.

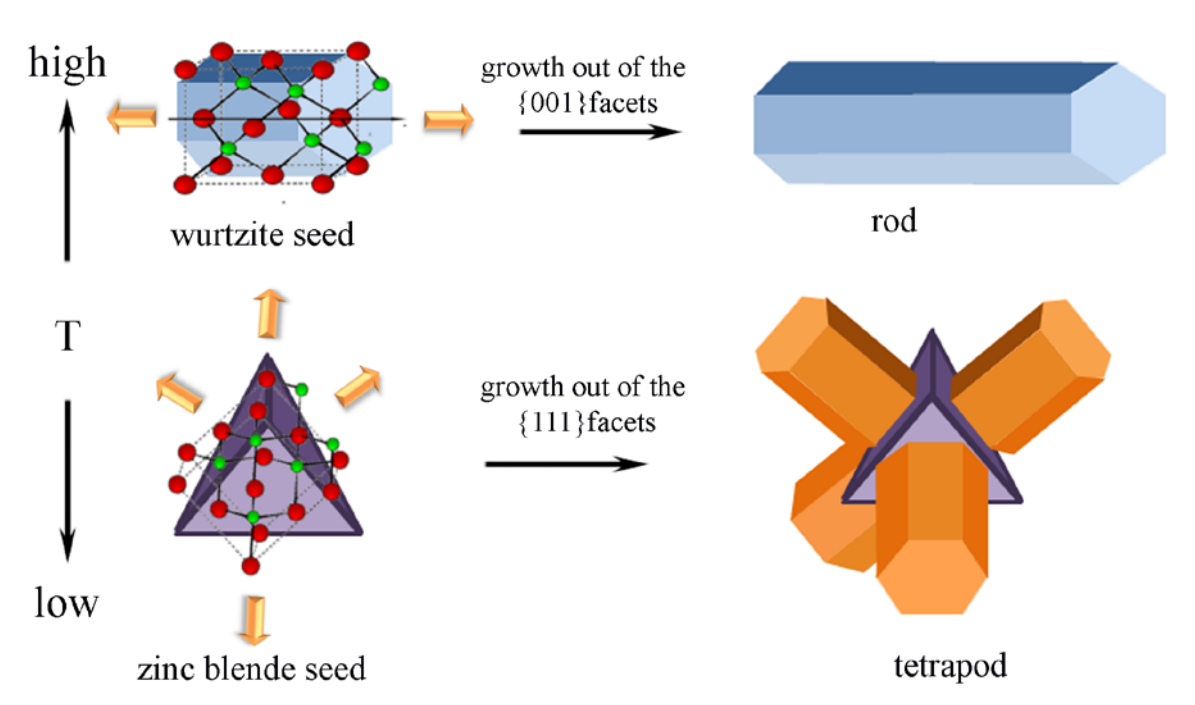


Figure 2.7 Temperature-mediated crystal-phase control of CdS nanocrystals: at low temperature tetrapods from zinc blende seeds are obtained, while at higher temperature only nanorods form starting from wurtzite seeds (adapted from ref. 4)

Therefore, the facets characterized by a high surface energy will grow faster, until they may eventually disappear to lower the overall NC formation energy.

Nevertheless, in colloidal system a further complication arises from the presence of surfactants that can act as selective adhering species that may be prone to a facet-preferential adsorption and selective stabilization.^{36, 41-43} Such action can influence the relative growth rates of specific crystalline facets and, consequently, the final NC shape, when the system is kinetically controlled.

The one-dimensional shape evolution of TiO₂ anatase NCs can be considered as an example.⁴² TiO₂ anatase has a tetragonal structure and has been shown to nucleate as truncated octahedral bipyramidal seeds, exposing eight equivalent {101}/{011} facets and two equivalent {001} facets with higher surface energy.⁴² The intrinsically higher reactivity of the {001} facets will lead to the formation of bullet and diamond-shaped NCs in which such facets are completely suppressed. When organic acid molecules, such as of lauric acid, are involved in the synthesis as capping agents, they will modulate the relative reactivity of the {101} and {001} facets by binding selectively to the latter. On increasing the lauric acid concentration in the reaction medium, NC growth along the {001} facets tends to be inhibited, until branched nanostructures results from crystal development out of the equivalent {101} facets of the bipyramidal seeds.⁴²

2.7 The seeded-growth approach to colloidal multi-material nanocrystals

"Seeded growth" relies on performing preferential heterogeneous nucleation and growth of secondary materials on preformed catalyst NC seeds, while avoiding undesired homogeneous nucleation in the bulk solution,. This approach is certainly one of the most effective strategies for the high-yield preparation of NC-based heterostructures, namely HNCs incorporating sections of different materials (§ 1.4). In general, it is hard to predict what topological configuration two or more different materials will take when attempting to combine them in a unique HNC particle.

In fact, a complex interplay of many factors, such as lattice compatibility, interfacial strain, materials miscibility, facet-dependent chemical reactivity, and changes in surface tension induced by adhesion of surfactants or ligands, should be taken in account. Examples of HNCs with different topological distribution of their component material sections are given in **Figure 2.8.** It is helpful to consider that the creation of HNC architectures by seeded growth in the solution phase share some similarities with the more traditional heteroepitaxial deposition processes accomplished by the Molecular Beam Epitaxy (MBE) and Chemical Vapour Deposition (CVD) techniques.

The sketch in **Fig. 2.9** illustrates this analogy by depicting the different modes in which a secondary material (2) can grow on a pre-existing substrate (1) of a different material. The ultimate growth mode will depend on the energy balance between the respective surface energies, σ_1 and σ_2 , and the solid-solid interfacial energy, $\gamma_{1,2}$, which is related to the mismatch between the two lattices. The change in total surface energy $\Delta \gamma$ that accompanies the deposition process is given by the equation:

$$\Delta \gamma = \sigma_1 - (\sigma_2 + \gamma_{1,2}) \tag{2.11}$$

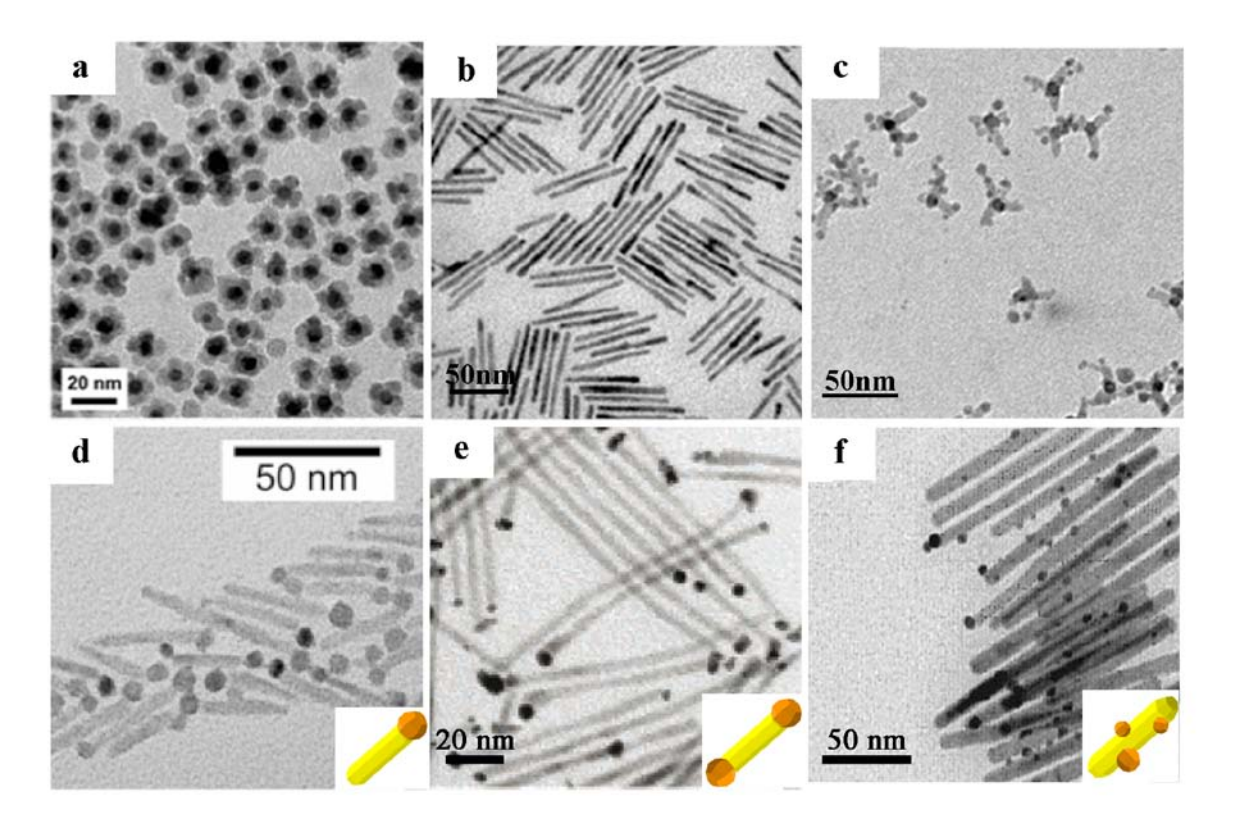


Figure 2.8. TEM examples of HNCs with different topological distribution of their component material sections, obtained by seeded growth.(a) Flower-like Au-Fe₃O₄ HNCs(from ref. 47); (b) asymmetric CdSe@CdS HNCs obtained by growing a rod-like CdS shell onto spherical CdSe seeds (from ref. 48) (c) Iron oxide tetrapods with cobalt tips (from ref. 49); (d) CdS nanorods with a PbSe tip in a matchstick-like configuration (from ref. 50); (b) dumbbell-like HNCs consisting of CdS nanorods with PtCo domains at both tips (from ref. 51); (c) non-selective gold-decorated Co nanorods (from ref. 52)

Three possible situations can take place, depending on the sign of $\Delta \gamma$. When the material (2) to be grown has a lower surface energy ($\sigma_2 < \sigma_1$) and the misfit between the two lattices is low (hence $\gamma_{1,2}$ is low) the deposition process results in a decrease in total surface energy. Therefore, the overgrowth of a homogeneous layer of (2) and formation of an extended interface between (1) and (2) are favored (*Frank-van der Merwe* mode in **Fig. 2.9a**). Differently, when the secondary material is characterized by a higher surface energy ($\sigma_2 < \sigma_1$) and/or the mismatch between the two materials is significantly high (γ_{12} is high), (2) can grow on (1) by forming discontinuous island-like domains, which allows the interfacial energy term to be minimized (*Volmer-Weber* mode in **Fig. 2.9b**). Another possibility resides in a mixed growth mode, which begins with the formation of a homogeneous film of (2) and then continues into the formation of islands as a means of reducing the interfacial strain tha intensifies along the deposition course (*Stranski- Krastanov* mode in **Fig. 2.9c**).

It is worth mentioning that, in wet-chemical synthesis, differently from CVD/MBE approaches, the growth modes of HNCs are strongly influenced by the presence of surface-adhering species (surfactants, ligands) that can indeed alter the surface energy terms considerably. 44-46

Another aspect that differentiates colloidal seeded growth from CVD/MBE approaches is that the conditions under which $\Delta \gamma > 0$ can be fulfilled either for all the exposed facets of the seed material or for a few of them, which corresponds to the formation of core@shell and dimer-like configurations, respectively (Fig. 2.9d).

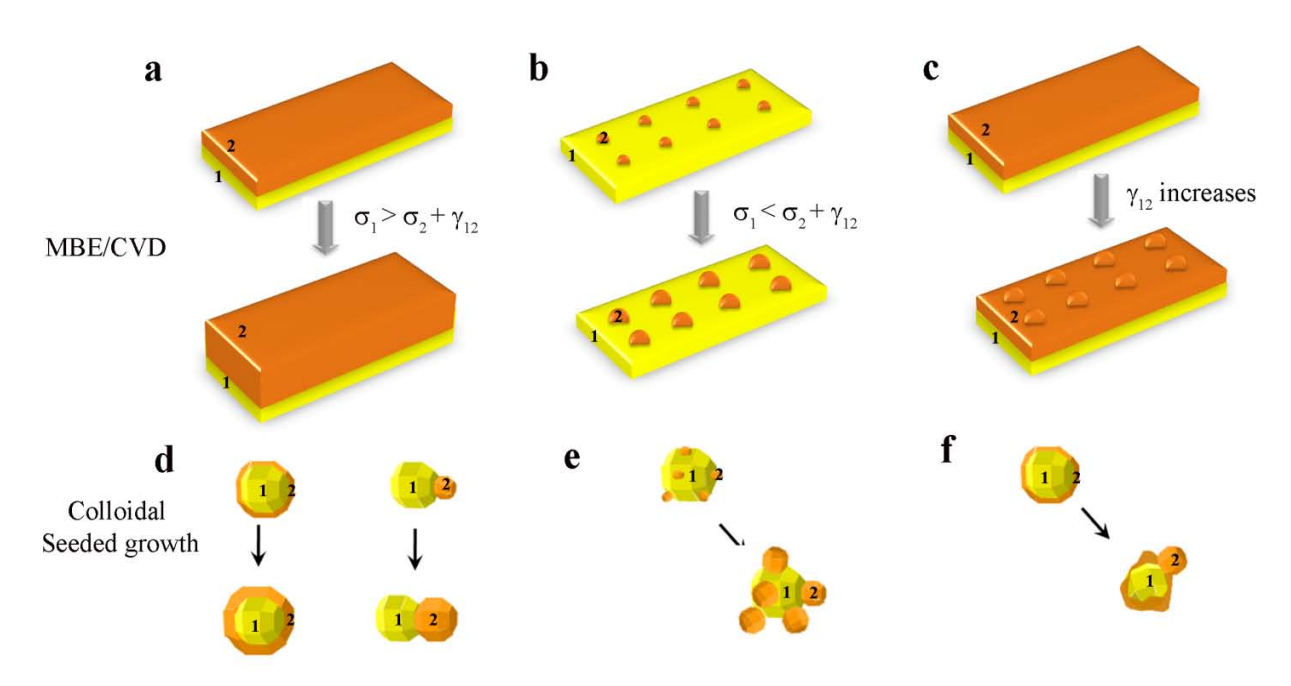


Figure 2.9 Comparative sketches depicting a parallelism among heterogeneous growth modes accomplished by MBE/CVD techniques (a-c) and seeded growth approaches in the solution phase (d-f), respectively

Moreover, in conditions of incomplete wetting ($\Delta \gamma < 0$), the growth of multiple secondary sections of the additional material can be achieved, provided that the seeds have sufficiently extended facets (**Fig. 2.9e**). As an intermediate case, it has been observed that HNCs initially attaining a core@shell configuration can successively evolve to hetero-dimers as phase segregation of the two material sections into discrete domains allows interfacial strain to be alleviated (**Fig. 2.9f**).

We have to consider that differently shaped NCs can be used as nucleation seeds. (**Fig. 2.8**). When nanorods are used to this aim, the nucleation of the second material could occur either at the tips or at the sidewalls, depending on the driving force of the heterogeneous growth mode (**Fig. 2.8d-f**). Actually, consistent with the anisotropic growth mechanism of rod-shaped NCs, the tips of the nanorods seeds frequently exhibit a higher reactivity, which offers the possibility to achieve preferential nucleation at these locations whenever the intervening interfacial strain maintains low enough. Moreover, when the basal facets of nanorods are crystallographically dissimilar, selective heterogeneous nucleation on one tip only may be achieved (**Fig. 2.8d**). ^{50, 51, 53-56}

References

- 1. Jun, Y.-w.; Choi, J.-s., C.; Cheon, J. Angew. Chem. Int. Ed. 2006, 45, 3414-3439.
- 2. Yin, Y.; Alivisatos, A.P. *Nature* **2005**, 437, 664-670
- 3. Lee, S. M.; Cho, S. N.; Cheon, J. Adv. Mater. 2003, 15, 441-444.
- 4. Jun, Y.-w.; Lee, J.-H.; Choi, J.-s.; Cheon, J. J. Phys. Chem. B 2005, 109,14795-14806.
- 5. Manna, L.; Kudera, S., Major mechanisms underlying the size and shape control of inorganic nanoparticles in the liquid phase. In *Advanced Wet-chemical Synthetic Approaches to Inorganic Nanostructures*, Cozzoli, P. D., Ed. Transworld Research Network: Kerala, India, 2008.
- 6. Hyeon, T. Chem. Commun. 2003, 8, 927-934.
- 7. Donega, C.D.; Liljeroth, P.; Vanmaekelbergh, D. *Small* **2005**, 1, 1152-1162.

- 8. Kwon, S.G.; Piao, Y.; Park, J.; Angappane, S.; Jo, Y.; Hwang, N.-M.; Park, J.-G.; Hyeon, T. *J. Am. Chem. Soc.* **2007**, 129, 12571-12584.
- Kobayashi, M.; Tomita, K.; Petrykin, V.; Yoshimura, M.; Kakihana, M. J. Mater. Sci. 2008, 432158 -2162.
- Buonsanti, R.; Grillo, V.; Carlino, E.; Giannini, C.; Kipp, T.; Cingolani, R.; Cozzoli, P.D. J. Am. Chem. Soc. 2008, 130,11223.
- 11. Stowell, C.A.; Korgel, B. Nano Lett. 2005, 5, 1203-1207.
- 12. Li, Y.; El-Sayed, M. A. J. Phys. Chem. B 2001, 105, 8938-8943.
- 13. Daou, T. J.; Grenèche, J. M.; Pourroy, G.; Buathong, S.; Derory A.; Ulhaq-Bouillet, C.; Donnio, B.; Guillon, D.; Begin-Colin, S. *Chem. Mater.* **2008**, 20, 5869-5875.
- 14. Klimov, V., Semiconductor and Metal Nanocrystals: Synthesis and Electronic and Optical Properties. 2007: Taylor & Francis.
- 15. Auer, S.; Frenkel, D. *Nature* **2001**, 409,1020-1023.
- 16. Park, J.; Joo, J.; Kwon, S. G.; Jang, Y.; Hyeon, T. Angew. Chem. In. Ed. 2007, 46, 4630-4660.
- 17. Shevchenko, E.; Talapin, D. V.; Schnablegger, H.; Kornowski, A.; Festin, O.; Svedlindh, P.; Haase, M.; Weller, H. J. Am. Chem. Soc. 2003, 125, 9090-9101.
- 18. Casula, M.F.; Jun, Y.W.; Zaziski, D. J.; Chan, E. M.; Corrias, A.; Alivisatos, A.P. *J. Am. Chem. Soc.* **2006**, 128,1675-1682.
- 19. Kwon, S.G.; Hyeon, T. Acc. Chem. Res. 2008, 41, 1696-1709.
- 20. Park, J.A., K.; Hwang, Y.; Park, J.-G.; Noh, H.-J.; Kim, J.-Y.; Park, J.-H.; Hwang, N.-M.; Hyeon, T. *Nat. Mater.* **2004**, 3, 891-895.
- 21. Park, J.; Lee, E.; Hwang, N.M.; Kang, M.; Kim, S. C.; Hwang, Y.; Park, J.-G.; Noh, H.-J.; Kim, J.-Y.; Park, J.-H.; Hyeon, T. *Angew. Chem. Int. Ed.* **2005**, 44, 2872-2877.
- 22. Joo, J.; Na, H. B.; Yu, T.; Yu, J. H.; Kim, Y. W.; Wu, F.; Zhang, J. Z.; Hyeon, T. J. Am. Chem. Soc. **2003**, 125, 11100-11105.
- 23. Roca, A. G.; Marco, J. F.; Morales, M.; Serna, C. J. J. Phys. Chem. C 2007, 111,18577-18584.
- 24. Sun, S. H.; Zeng, H.; Robinson, D. B.; Raoux, S.; Rice, P. M.; Wang, S. X.; Li, G. X. *J. Am. Chem. Soc.* **2004**, 126, 273-279.
- 25. Sun, S.; Zheng, H. J. Am. Chem. Soc. 2002, 124, 8204-8205.
- 26. Pradhan, N.; Reifsnyder, D.; Xie, R.; Aldana, J.; Peng, X. J. Am. Chem. Soc. 2007, 129, 9500-9509.
- 27. Murray, C.B.; Norris, D.J.; Bawendi, M.G. J. Am. Chem. Soc. 1993, 115, 8706-8715.
- 28. Kim, Y. H.; Jun, Y. W.; Jun, B. H.; Lee, S. M.; Cheon, J. W. J. Am. Chem. Soc. 2002, 124,13656-13657.
- 29. Green, M. Chem. Commun. 2005, 3002-3011.
- Ahrenstorf, K.; Heller, H.; Kornowski, A.; Broekaert, J.; Weller, H. Adv. Funct. Mater. 2008, 18, 3850-3856.
- 31. Sau, T.; Rogach, A. Adv. Mater. 2009, DOI: 10.1002/adma.200901271
- 32. Tao, A.; Habas, S.; Peidong, Y. Small 2008, 4, 310-325.
- 33. Bao, N.; Shen, L.; An, W.; Padhan, P.; Heath Turner, C.; Gupta, A. Chem. Mater. 2009, 21, 3458.
- 34. Liu, L.; Zhuang, Z.; Xie, T.; Wang, Y.-G.; Li, J.; Peng, Q.; Li, Y. J. Am. Chem. Soc. 2009, 131,16423-16429.
- 35. Kim, D.; Lee, N.; Park, M.; Kim, B. H.; An, K.; Hyeon, T. J. Am. Chem. Soc. 2009, 131, 454-455.
- 36. Xiong, Y.; Xia, Y. Adv. Mater. 2007, 19, 3385-3391.
- 37. Zhang, J.; Sun, K.; Kumbhar, A.; Fang, J. J Phys. Chem. C 2008, 112, 5454-5458.
- 38. Xia, Y.; Xiong, Y.; Lim, B.; Skrabalak, S. Angew. Chem. Int. Ed. 2009, 48, 60-103.
- 39. Jun, Y.-w.; Lee, S.M.; Kang, N.J.; Cheon, J. J. Am. Chem. Soc. 2001, 123, 5150-5151.
- 40. Gong, X. Q.; Selloni, A. Phys. Rev. B 2007, 76, 23.
- 41. Peng, X.; Manna, L.; Yang, W.; Wickham, J.; Scher, E.; Kadavanich, A.; Alivisatos, A. P. *Nature* **2000**, 404, 59-61.
- 42. Jun, Y. W.; Casula, M. F.; Sim, J. H.; Kim, S. Y.; Cheon, J.; Alivisatos, A. P J. Am. Chem. Soc. 2003, 125, 15981-15985.
- 43. Jamie, H.W.; Huaqiang, C. *Nanotechnology* **2008**, 19, 305605.
- 44. Cozzoli, P.D.; Pellegrino, T.; Manna, L. Chem. Soc. Rev. 2006, 35, 1195-1208.
- 45. Buonsanti, R.; Casavola, M.; Caputo, G.; Cozzoli, P. D. Recent Pat. Nanotechnol. 2007, 1, 224-232.
- 46. Casavola, M.; Buonsanti, R.; Caputo, G.; Cozzoli P.D. Eur. J. Inorg. Chem. 2008, 837-854.
- 47. Yu, H.; Chen, M.; Rice, P. M.; Wang, S.X.; White, R. L.; Sun, S. Nano Lett. 2005, 5, 379-382.
- 48. Carbone, L.; Nobile, C.; De Giorgi, M.; Della Sala, F.; Morello, G.; Pompa, P.; Hytch, M.; Snoeck, E.; Fiore, A.; Franchini, I.R.; Nadasan, M.; Figuerola, A.; Chiodo, L.; Kudera, S., Cingolani, R.; Krahne, R.; Manna, L. *Nano Lett.* **2007**, 7, 2942-2950.
- 49. Casavola, M.; Falqui, A.; Garcia, M. A.; Garcia-Hernandez, M.; Giannini, C.; Cingolani, R.; Cozzoli, P.D. *Nano Lett.* **2009**, 9, 366-376.
- 50. Kudera, S.; Carbone, L.; Casula, M. F.; Cingolani, R.; Falqui, A.; Snoeck, E.; Parak, W. J.; Manna, L. *Nano Lett.* **2005**, 5, 445-449.

- 51. Habas, S.; Peidong, Y.; Mokari, T. J. Am. Chem. Soc. 2008, 130, 3294-3295.
- 52. Wetz, F.; Soulantica, K.; Falqui, A.; Respaud, M.; Snoeck, E.; Chaudret, B. Angew. Chem. Int. Ed. 2007, 46, 7079-7081.
- 53. Elmalem, E.; Saunders, A.; Costi, R.; Salant, A.; Banin, U. Adv. Mater. 2008, 20, 4312-4317.
- Mokari, T.; Sztrum, C. G.; Salant, A.; Rabani, E.; Banin, U. Nat. Mater. 2005, 4, 855-863. 54.
- 55. Maynadié, J.; Salant, A.; Falqui, A.; Respaund, M.; Shaviv, E.; Banin, U.; Soulantica, K.; Chaudret, B. Angew. Chem. Int. Ed. 2009, 48,1814-1817.
- 56. Pacholski, C.; Kornowski, A.; Weller, H. Angew. Chem. Int. Ed. 2004, 43, 4774-4777.